Cardiovascular Engineering and Technology, Vol. 14, No. 1, February 2023 (© 2022) pp. 37–51
https://doi.org/10.1007/s13239-022-00637-z

Original Article

Development of Multifunctional Commercial Pure Titanium-Polyethylene Glycol Drug-Eluting Substrates with Enhanced Optical and Antithrombotic Properties

MONALISHA MOHANTA[1] and A. THIRUGNANAM[2]

[1]Department of Biotechnology and Medical Engineering, National Institute of Technology Rourkela, Rourkela, Odisha 769008, India; and [2]Department of Biotechnology & Medical Engineering, National Institute of Technology Rourkela, Room No. 206, Rourkela, Odisha 769008, India

(*Received 23 April 2021; accepted 2 June 2022; published online 14 June 2022*)

Associate Editor Roozbeh Ghaffari oversaw the review of this article.

Abstract
Purpose—Development of multifunctional advanced stent implants (metal/polymer composite)—drug-eluting stents with superior material and optical properties is still a challenge. In this research work, multifunctional metal-polymer composite drug-eluting substrates (DES) for stent application were developed by using commercially pure titanium (cpTi) and polyethylene glycol (PEG).
Methods—Surface modifications on titanium substrates were carried out by sodium hydroxide under various concentrations; 5M (6 and 24 h) and 10M (6 and 24 h). It induces a nanoporous structure which facilitates the larger area for encapsulation of the drug, Aspirin (ASA) *via* intermolecular forces followed by polymer coating of PEG (MW-20,000) by physical adsorption process, which is structured as layer-by-layer gathering.
Results—The developed cpTi-PEG DES were characterized using X-ray diffraction (XRD), Fourier transform infrared spectroscopy (FTIR), scanning electron microscopy (SEM), optical energy bandgap, static contact angle measurement, antithrombotic and drug release studies. The development of sodium titanate oxide prompted surface nano-features revealed by SEM and XRD. Moreover, FTIR confirms the presence of ASA and PEG functional groups over the cpTi surface. Drug release studies fitted with Ritger–Peppas kinetic model (≤ 60%), which indicates the super case II transport mechanisms ($n > 1$). Further UV–visible absorbance spectrum was quantified by the Tauc plot, which shows the broadening of the energy bandgap (E_g). In addition, the shrink in blood clots was more around the Tib2/ASA/PEG.
Conclusion— Developed cpTi-PEG DES has improved optical properties and prevent thrombus formation which suggesting it a potential substrate to overcome prime clinical challenges.

Keywords—Surface nano-features, Titanium, Optical energy bandgap, Drug release kinetic, Antithrombosis.

INTRODUCTION

Multifunctional materials were a promising candidate for various cardiovascular implants like valve replacement, stents implants, catheters, *etc*. Developing bio-engineered composite stent material with advanced properties to fulfill the clinical need is still a challenge. Much research on drug-eluting stents focuses mainly on refined structural properties—integrity, design, anti-corrosion, antithrombotic nature, hemocompatibility, and drug-releasing profiles along with post clinical investigation.[37,48] Furthermore, drug-eluting stents implants usually fabricated using stainless steel, cobalt–chromium, and titanium alloys.[27,54,69,73] The major drawback of these stent materials is a concern in developing multifunctional bio-engineered novel metal-polymer composite drug-eluting substrates (DES) with superior properties overcoming specific issues like thrombosis, an immunogenic reaction caused by alloys, and the challenges faced in the micro-environment inside the blood vessel.[74] It is seen that the biocompatibility of 316L stainless steel (SS) remains stringent because of thrombosis formation.[55] As far as stents made up of nitinol (NiTi) alloy has, more concern exists over the nickel leakage, which causes immunogenic reaction

Address correspondence to A. Thirugnanam, Department of Biotechnology & Medical Engineering, National Institute of Technology Rourkela, Room No. 206, Rourkela, Odisha 769008, India. Electronic mail: thirugnanam.a@nitrkl.ac.in

leading to toxicity.[72] Commercially pure titanium (cpTi) and its composites are generally considered in the therapeutic embed because of magnificent biocompatibility and excellent mechanical properties, enabling it as multifunctional material satisfying the needs of an advanced material with versatile applications like dental, orthopedic inserts, and cardiac implants.[14,59,66] In addition, Titanium (Ti) possesses a low modulus of elasticity that makes it highly flexible.[15] However, cpTi has a poor radiopaque property which acts as a barrier in the post-clinical identification of Ti implants.[45] Stents made from a cobalt–chromium alloy and tantalum, although showing better radiopaque properties still have few limitations due to stent thrombosis, inflammation, and biocompatibility.[8,52] Like pre-clinical challenges faced during the development of implant materials like stents, post-clinical testing is another area where significant difficulties are confronted.[51] So, to overcome the problem related to the post clinical identification and thrombosis formation, metal-polymer stent composite DES has been introduced, which has supreme advantages such as control drug release and prolongation of these implants in the micro-environment, which prevents thrombosis development when compared to bare metallic stents and also enhances its mechanical strength.[49] Few studies have reported metal-polymer stent composite optical properties, which might be an essential study in post-clinical identification.

Polymers such as polyvinyl alcohol, polyethylene glycol (PEG), poly-lactic-co-glycolic acid and poly-L-lactide acid, *etc*., are promising polymeric candidates for DES to enhance the performance.[58] The PEG is a biodegradable, biocompatible, and FDA-authorized polymer widely used for drug delivery.[44] PEGs are also termed Macrogol. It is a polyether made out of rehashed ethylene glycol units. Commercially available PEGs are accessible with various degrees of polymerization and activated efficient groups. The high extremity of PEG expands hydrophilicity and, in this manner, upgrades water solvency, a distinctive element among the comparable auxiliary polymers.[6] Also, PEG increases the hydrophilic nature of the stents due to its polyester group.[47] PEG-based polymers are significant in some fields, such as cell and tissue designing, biosensors, and medicate conveyance systems. Specifically, PEG coatings have been widely used to limit vague fouling of the surfaces with plasma proteins or to produce a form of proteins or cells.[18,29,60] The polymer framework influences the drug discharge profiles by lessening medication draining through the polymeric grids or developing a broke up drug through the polymeric networks.[4,62] Some studies on the PEG polymer matrix confirmed that it has the potential to enhance optical properties.[2] Imaging the metal-polymer composites implant by X-ray, MR, and fluoroscopy imaging is still a more significant challenge due to the material properties, fabrication, and design. Stents, a catheter made up of nitinol alloy, copper, or plastic implants, are less vulnerable through these imaging techniques. Commonly, iron, gold, and dysprosium (rare earth elements) are used as markers for better tracking and visualization of these endovascular implants.[16]

The present study focuses on the drug-eluting substrate developed from cpTi-PEG composite because cpTi and PEG have better biocompatibility properties, as discussed above. The drug utilized for this research is acetylsalicylic acid (Aspirin, ASA), which is considered an anticoagulant used for entrenched treatment for the aversion of cardiovascular diseases.[32] This study employed a PEG of high molecular weight of 20,000 to coat the dug surface. It is considered an antifouling agent, and the glass transition temperature is about − 22.37 °C with a melting point of 51 °C.[67] The graphic illustration of the synthetic itinerary of the developed composites by a layer-by-layer process is represented in Fig. 1. The surface treatment is one of the critical processing parameters in material development, which enhances an implant's surface adhesion properties, leading to better performance.[31] Therefore, the surface modification with alkali treatment generates a –OH hydroxyl group which facilitates the ionic connection among the acetylsalicylic acid (Aspirin, ASA), synthetic polymer, and the metal (Si) substrate. Extensive studies were done with alkali treatment, which shows sodium titanate oxide over the surface, improving the surface features. The PEG polymer network over the drug-loaded cpTi substrates plays a vital parameter in eluting the drug. Therefore, the cpTi surface is modified by alkali treatment with NaOH, allowing it to withhold the polymer (PEG) and drug (ASA) layers, making it a better DES. It was observed that alkali concentration and treatment time had modified the surface of the cpTi substrate. It has influenced nanostructure formation on cpTi substrates, which enhances medication embodiment and polymers coating leading to the development of cpTi/ASA/PEG DES with better performances which were investigated by Scanning electron microscope (SEM), X-ray diffraction (XRD), Fourier transform infrared radiation (FTIR), static water contact angle measurement (CAM) and optical energy band gap respectively. The controlled drug release studies were done using Ritger–Peppas mathematical equations kinetic model. Further, the *in-vitro* antithrombotic analysis of the modified surfaces was performed in provisos of blood cluster mass. The optical energy band gap of cpTi/ASA/PEG shows an optical band edges enhancement where the edges are shifting towards higher energy (red

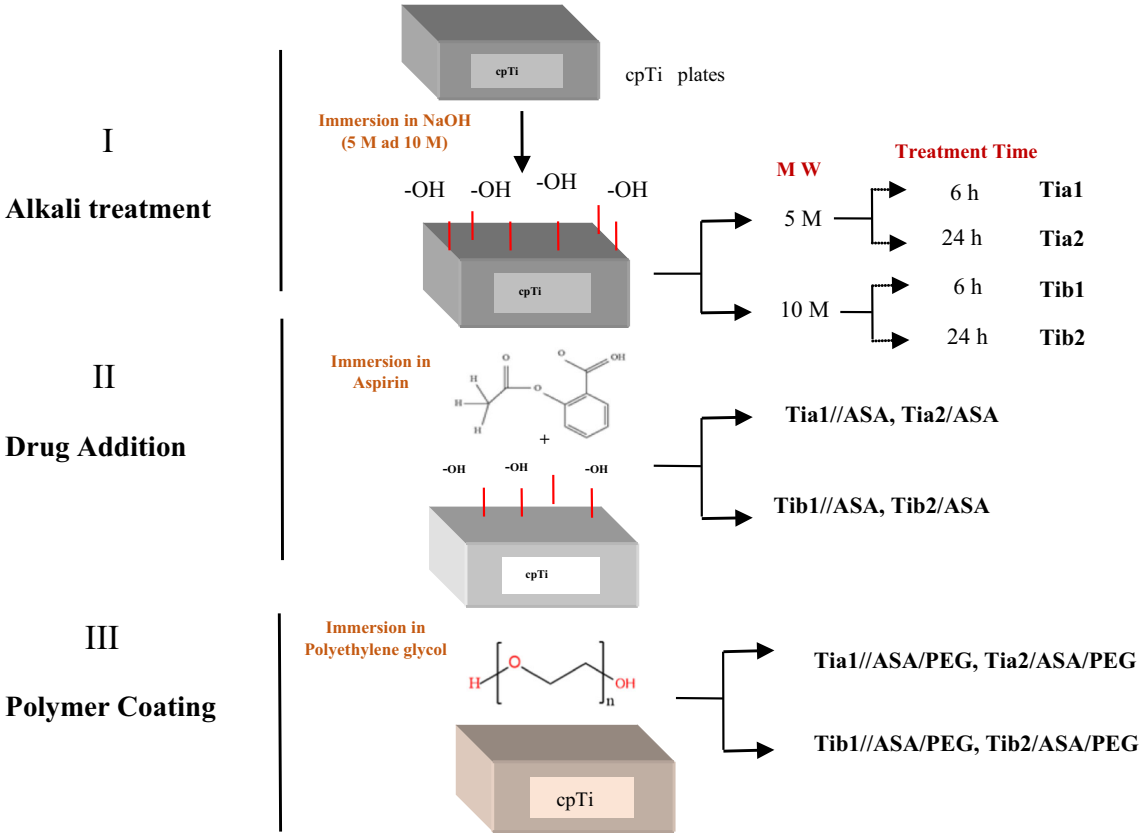

FIGURE 1. Schematic demonstration of synthetic itinerary of Tia1/ASA/PEG, Tia2/ASA/PEG, Tib1/ASA/PEG, and Tib2/ASA/PEG on cpTi substrate *via* layer-by-layer process.

shift) because of the broadening of the energy band gap. Hence, surface treatment has not only enhanced the surface properties but also the optical characteristic of the cpTi DES which may assist to enable in post clinical identification of stents.

MATERIALS AND METHODS

Materials Required

Commercially pure titanium (cpTi) was bought from MIDHANI (Mishra Dhatu Nigam Limited, India), Hyderabad, India. Aspirin (ASA (acetylsalicylic acid)) of 75 mg (manufactured by USV Pvt. Ltd., India) as FDA approved was purchased from the government medical shop. Hydrofluoric acid (HF) (40%, 1.93414.0521-500 mL), nitric acid (HNO_3) (70% pure, AS008-500 mL), hydrogen peroxide (H_2O_2) (PCT1511-500 mL), acetone (C_3H_6O) (AS024-500 mL), and sodium hydroxide (NaOH) (RM467-500G) chemicals were procured from Hi-Media laboratories Private Limited, India. Sodium hydroxide (NaOH) [RM467-500G] and calcium chloride ($CaCl_2$) [499609-1G] were purchased from Sigma Aldrich, India. Polyethylene glycol (PEG, 20000) [25322-68-3] was procured from SRL Private Limited, India. Goat blood was collected from the local butcher shop.

METHODS

Alkali Treatment

Commercially pure titanium (cpTi) plates were cut into small dimensions of 1 × 1 cm of thickness 0.8 mm. These small plates were chemically cleaned in an acid solution containing HF, HNO_3, and H_2O_2 at a specified proportion (1:3:5) for 5 min followed by ultrasonically washing with acetone, alcohol, and deionized water for 15 min and later dried in a hot air oven at 37 °C.[25,41] After drying, cpTi plates were immersed in 5 M and 10 M NaOH solution for 6 h and 24 h at 60 °C in a water bath. The samples were taken out later, followed by rinsing with distilled water, and dried at 37 °C.

Development of DES

Drug encapsulation over the alkali-treated cpTi substrates was carried out by soaking the plates in acetylsalicylic acid (Aspirin) solution (50 and 150 mg dose) for 12 h at 37 °C by immersion method. The

soaked cpTi plates were taken out, rinsed with distilled water, and dried at 37 °C. Subsequently, the cpTi substrates with Aspirin were soaked in 1% w/v (optimized) of a lubricious polymer PEG (MW-20,000) solution at 37 °C for 2 h. Again, the developed DES substrates were taken out, followed by rinsing with distilled water and dried. The developed composite was simple one layered stacked DES[75] and treated at body temperature. The followed experimental technique was rehashed three times. The overall protocols, along with substrates code, are shown in Table 1.

Surface Characterization

Structural modification of alkali-treated cpTi (Tia1, Tia2, Tib1, and Tib2) was analyzed by X-ray diffraction (XRD, X-Pert, PANalytical, PW 3040/00, Netherlands). The surface morphology of Ti, Tia1, Tia2, Tib1, Tib2, Tia1/ASA, Tia2/ASA, Tib1/ASA, Tib2/ASA, Tia1/ASA/PEG, Tia2/ASA/PEG, Tib1/ASA/PEG, and Tib2/ASA/PEG was analyzed by scanning electron microscopy (SEM: JEOL, JSM-6480 LV, EDS.: Oxford Instruments, Netherlands). The SEM micrographs are recorded at a magnification of × 80,000, on a 2 μm scale with an accelerating voltage (HV) of 15.00 KV. The pore size was measured using Image J software. The surface hydrophilicity of DES samples was investigated using the sessile drop technique using the Drop shape analyzer, contact angle (Kruss, DSA 25, Germany) as 3 μL of deionized water was dropped to the modified surface to quantify the water contact point at room temperature. The optical band gap measurements were carried out for the Ti, Tia1, Tia2, Tib1, Tib2, Tia1/ASA, Tib1/ASA, Tia2/ASA/PEG, and Tib2/ASA/PEG in UV–visible spectrofluorometer (UV-2450 spectrofluorometer, Shimadzu, Japan). The obtained energy bandgap (E_g) was calculated by the Tauc Plot method. The molecular bonding of alkali-treated Ti (Tia1, Tia2, Tib1, and Tib2) and Aspirin molecular bonding with the alkali-treated sample (Tia1/ASA, Tia2/ASA, Tib1/ASA, and Tib2/ASA) was resolved by Fourier transform infrared spectroscopy (FTIR-ATR, Shimadzu, IR prestige-21, Automatic infrared microscope, Japan). The drug (ASA) release experiments done in PBS (pH 7.4) and antithrombotic studies were analyzed by a UV–visible spectrophotometer.

Drug Release Kinetic

Increasing the performance of stent implants in sustainable drug release polymer coatings plays a significant role, thereby enhancing the efficiency as a composite material.[3,9,24] The alkali-treated cpTi were further coated with a drug (Aspirin, ASA) of both 50 and 150 mg. Moreover, the coated PEG polymer was used to control the discharge rate of the drug. The *in-vitro* drug elution study was done for Tia1/ASA/PEG, Tia2/ASA/PEG, Tib1/ASA/PEG, and Tib2/ASA/PEG sample in 2 mL of phosphate buffer saline (PBS) of pH 7.4 and incubated at 37 °C in an incubator shaker at 100 rpm. The quantity of drug release was analyzed in a UV–visible spectrophotometer (systronics double beam spectrophotometer 2203), and absorbance was taken at 275 nm.[30] The experiment was repeated three times.

Investigation of the Aspirin (ASA) release kinetic from the cpTi substrates was performed by fitting the test information to the Ritger–Peppas represented Eq. (1):

$$F = \frac{M_t}{M_\infty} = kt^n \tag{1}$$

where M_t/M_∞ is the fractional drug (Aspirin) release, k is considered kinetic constant, and n is the diffusion exponent, which identifies the drug release pattern from the transport system. The nature of diffusion identified by $n = 1$ (case II transport, prompting a zero-order discharge profile.), $n > 1$ (super case II transport), $n = 0.5$ (Fickian diffusion), and $0.5 < n <$

TABLE 1. Chemical treatments and encapsulation of molecules employed over the cpTi substrates.

Sample code	Treatment stipulation	Facts of treatment
Ti	Untreated	Only chemically clean cpTi with HF, HNO_3 and H_2O_2
Tia1	NaOH treated	5 M NaOH for 6 h
Tia2		5 M NaOH for 24 h
Tib1		10 M NaOH for 6 h
Tib2		10 M NaOH for 24 h
Tia1/ASA,Tia2/ASA,Tib1/ASA and Tib2/ASA	Aspirin encapsulation	Tia1, Tia2,Tib1 and Tib2 samples were soaked in the aspirin solution for 2 h
Tia1/ASA/PEG,Tia2/ASA/PEG,Tib1/ASA/PEG and Tib2/ASA/PEG	PEG coating	Tia1/ASA, Tia2/ASA,Tib1/AS A and Tib2/ASA were soaked in PEG (MW-20,000) solution for 2 h

1 (non-fickian diffusion). This kinetic model is considerable for $M_t/M_\infty \leq 60\%$.[36,53] The Ritger–Peppas equation was mathematically calculated using the solver and data analysis (correlation) model in Microsoft excel.

Antithrombotic Assay

The antithrombotic assay of developed cpTi-DES was evaluated *in-vitro* by direct interaction with blood as per ASTM F756 standard.[61] It was carried out by dropping anticoagulated blood of 200 μL onto the sample surfaces, and 20 μL of 0.2 M calcium chloride was added to initiate coagulation. After 30 min of incubation at 37 °C and 30 r/min, the red blood cells (RBCs) that were not trapped in the clot were hemolyzed by pouring 25 mL distilled water slowly along the wall of the tube. The absorbance (OD) of the resulting hemoglobin solution was taken at 540 nm. Here, the whole blood was centrifuged at 1000 rpm for 30 min at 4 °C.[17]

Statistical Analysis

Every single quantitative result was performed by utilizing one-way single factor ANOVA. Information was analyzed as the mean ± SD. An estimation of $*p < 0.05$ and $**p < 0.005$ demonstrates significant differences.

RESULTS AND DISCUSSION

XRD Analysis

The XRD results revealed the formation of one-dimensional sodium titanate ($Na_2Ti_3O_7$) structures of the alkali-treated substrates in Fig. 3A. Strong diffraction peaks of sodium titanate oxides in Ta1, Ta2, Tb1, and Tb2 have been observed. Two prominent diffraction peaks, $2\theta \approx 47°$ and 62°, are related to the $Na_2Ti_3O_7$ (JCPDS card # 72-0148) form of titanates following the literature.[57] The intensity of these peaks for Tia2 and Tib2 (24 h treatments) are slightly higher than Tia1 and Tia2 (6 h treatments). This shows that the crystallinity of sodium titanate formation on alkali-treated samples increases with the treatment time. Moreover, it was observed that the sodium titanate oxide layer was more profoundly formed over 10 M-24 h alkali-treated (Tib2) substrate. A similar trend of prominent peaks with increasing concentration of NaOH was observed in the literature.[71] After forming the $Na_2Ti_3O_7$ layer, there is a possibility of the presence of Ti-OH groups on the substrate's surface.[50] The development of sodium titanate oxides was considered to have superior bioactivity.[26]

SEM Analysis

Micrographs of the alkali-treated cpTi substrates revealed the formation of nanoporous structures supporting the XRD, which justifies that the surface treatment can improve the surface nano-features of the substrate (cpTi) material which further aids in drug encapsulation, as shown in Fig. 2. These nanoporous structures correspond to the broadening of bandgap, leading to shifting in the absorption edge,[22] which was evident by optical bandgap studies. Surface geology shows a significant trade in the surface structure and interaction with the drugs.[33]

SEM micrographs have revealed the relation between alkali surface treatment and encapsulation of drugs. It has been observed that the pore size formation is better in 10M (Figs. 2g and 2j) alkali-treated cpTi substrate when compared to the 5 M cpTi (Figs. 2a and 2d). Moreover, improvement in the nano-pores formation was observed in 10 M-24 h (Tib2) alkali-treated substrate compared to 10 M-6 h (Tib1) alkali-treated cpTi substrates. Eventually, the increase in concentration and hours of alkali treatment has improved the surface nano-features of the substrate due to the formation of sodium titanate oxide, which is also reflected in the XRD. It has paved the scope for more aspirin encapsulation and PEG coating, thereby enabling Tib2 to perform as a better drug-eluting substrate (DES) in comparison with other alkali-treated drug-eluting substrates- Tia1 (5 M-6 h), Tia2 (5 M-24 h), and Tib1 (10 M-6 h). A similar trend, alkali treatment provides better scope for nanometer permeability, enhancement of morphology, and providing a better pores network topographical arrangements on cpTi surface, has been reported.[21,68] The partially filled white layer on the nanoporous surface confirmed better Aspirin encapsulation. Later, a thick layer of the polymer covered the entire Aspirin-contained modified surface (Figs. 2k and 2l). However, it was noticed that surface irregularities were minimized and homogenously layered all over the surface with PEG coating. Also, tiny narrow pores were present on the polymer layer. These microscopic pores help in controlling the rate of diffusion of the drug (Aspirin). The pore size of alkali-treated samples was calculated by Image J software, as shown in Table 2. It has been justified that the pore size has increased from 134.5 to 228.6 nm, increasing alkali concentration and treatment time, leading to more drug encapsulation. From this, it is evident that surface treatment plays a crucial parameter in the DES.

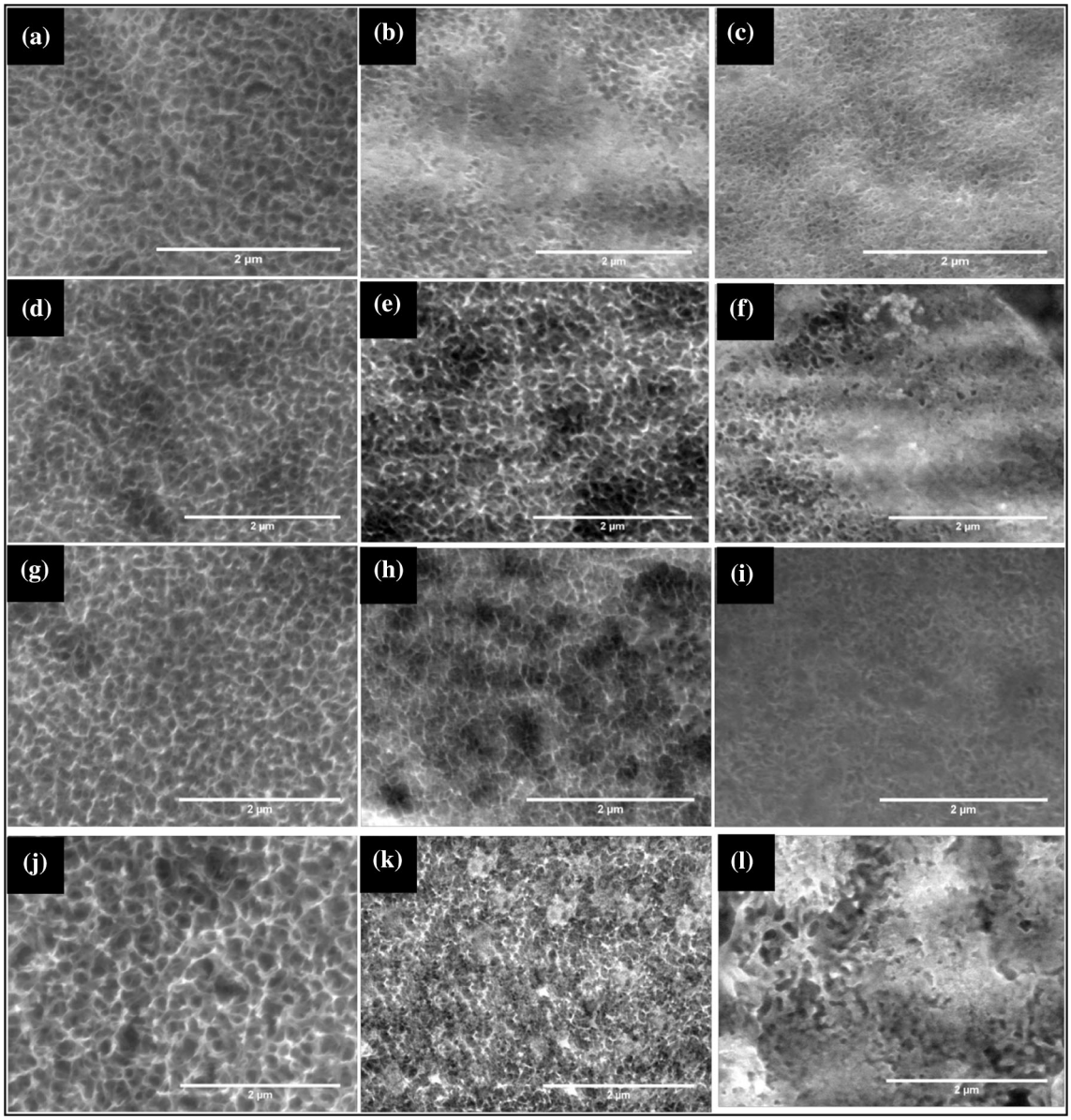

FIGURE 2. SEM micrographs of alkali-treated (NaOH) following with Aspirin (ASA) added and PEG coated cpTi substrates: (a) Tia1, (b) Tia1/ASA, (c) Tia1/ASA/PEG, (d) Tia2, (e) Tia2/ASA, (f) Tia2/ASA/PEG, (g) Tib1, (h) Tib1/ASA, (i) Tib1/ASA/PEG, (j) Tib2, (k) Tib2/ASA and (l) Tib2/ASA/PEG.

FTIR Analysis

Surface treatment processing parameters play a vital role in changing the morphology of pure cpTi substrates, which was evident from the SEM analysis. Following these FTIR spectra of alkali-treated substrates, aspirin-coated and PEG-coated sample has shown the presence of functional groups which act a vital role in the surface modification on Ti substrates which is illustrated in Figs. 3b and 3c. The band around the region 3600 cm^{-1} and 1636 cm^{-1} correspond to –OH stretching of weekly bound water, thereby proving the presence of Ti–OH or Ti=O groups. The peak found around 1061 cm^{-1} attributed to the bending vibration of H–O–Ti of the hydrotitanates. The FTIR spectrum of Tib2 substrate shows a feeble band at 875 cm^{-1} of Na–O twisting affirms the existence of sodium titanates (Na–O–Ti). Hence, FTIR spectra reconfirm the presence of sodium titanates which plays a vital role in improving the drug loading capability of alkali-treated Ti substrates. Further with the encapsulation of aspirin (ASA), the bands were found to occur around 1690 cm^{-1} and 1011 cm^{-1}, which is associated with C=O and C–O stretching of the ester group of aspirin.[7,56,64] Thus, the ASA functional group interacted with the NaOH treated cpTi

TABLE 2. Calculated average pore size of the different alkali-treated cpTi substrates, Variation in adsorption edge and energy band gap of the different alkali-treated, aspirin loaded and PEG-coated Ti substrates and calculated transmittance percentage (%T) and opacity value of cpTi-DES substrates from the absorbance, opacity and absorbance relationship.

M W		5M						10M					
Time (h)	Without	6 h			10 h			6 h			10 h		
Substrates	Ti	Tia1	Tia1/ ASA	Tia1/ ASA/ PEG	Tia2	Tia2/ ASA	Tia2/ ASA/ PEG	Tib1	Tib1/ ASA	Tib1/ ASA/ PEG	Tib2	Tib2/ ASA	Tib2/ ASA/ PEG
Average pore size (nm)		134.5			136.6			184.5			228.6		
Absorption edge (nm)	280	312	315	367	311	307	364	309	304	360	303	290	358
Energy band-gap (eV)	2.95	3.03	3.25	3.04	3.12	3.34	3.14	3.10	3.41	3.18	3.17	3.52	3.24
%T	20.8	20.4	11.7	19	11.5	10.0	17.4	10.7	9.33	16.6	10	8.0	16.0
Opacity	4.8	4.9	8.5	5.2	8.6	0.1	5.7	9.3	10.7	6.0	10	12.5	6.2

surface through intermolecular forces, particularly dipole–dipole intermolecular reaction because of the interaction between the two polar active groups.

The FTIR spectra of PEG (20,000)—coated substrates such as Tia1/ASA/PEG, Tia2/ASA/PEG, Tib1/ASA/PEG, and Tib2/ASA/PEG has shown in Fig. 3c. The peaks for the alkyl chain of PEG, C–H twisting, C–O extending vibration, and C–H winding vibrations are supposed to appear around 2888, 1342, 1100, and 1242 cm^{-1}.[23,43,65] However, in this study sharp peak of the alkyl chain was observed in the region of 2864 cm^{-1}. Peak Intensity at this band was observed high for Tib2/ASA/PEG compared to other samples. It may be due to formation of a large porous network in Tib2/ASA/PEG. The aforementioned functional groups of PEG affirm the physisorption coating of the polymer layer over the cpTi-ASA surface. Therefore, the FTIR spectra verified that alkali treatment played a vital role in enhancing the surface features of Ti substrates as the concentration and treatment time increases the intensity of bands found to increase. The presence of C = O stretching of aspirin is more prominent in the Tib2 (10 M-24 h) substrate. Moreover, a similar trend was observed in PEG-coated cpTi substrates.

Static Contact Angle Measurement

The improvement in the hydrophilic nature of Ti substrates before alkali treatment can be observed from the contact angle measurement as illustrated in Fig. 3d. Surface modification has played a critical role in enhancing the hydrophilic nature of Ti substrates, creating a nanoporous structure of sodium titanate featuring wettability, drug encapsulation, and elution. The measured contact angle for untreated Ti substrate is about 110 ± 0.01°, which is hydrophobic.

It has been noticed that NaOH treatment considerably reduces the contact angle to 12.4 ± 2.4°, 15.2 ± 3.3°, 24.6 ± 2.8° and 37.2 ± 3.6°, due to irregularities in the pore size distribution of sodium titanates throughout the surface owing to the concentration and treatment time.[1,28,34] The increase in the surface irregularities increases the surface energy, which thereby enhances the wettability of the substrate's surface. The hydrophilic behavior of the Ti substrate's surface also enhances the drug loading capability. The contact angle of drug-loaded polymer-coated substrates has also shown in Fig. 3d. It has been observed from contact angle measurement that Tia2/ASA/PEG (5 M-24 h) substrate, which is about 29.7 ± 1.5° wettability, is more as compared to Tib2/ASA/PEG (10 M-24 h) substrate, which is about 30.4 ± 2.1°. It may be due to a fascination with hydroxyl gathering changing the wettability of cpTi surfaces, as also substantiated by the above FTIR results.[11] This smooth, slippery polymer coating provides less friction between blood and substrate surfaces. The literature also reported that ASA contributes to the increase in the hydrophilic groups over the Ti substrate's surface.[10] Thus, the ASA-loaded and PEG-coated surfaces enhance the wettability of the surface, which can improve the cell viability percentage, thereby improving the biocompatibility of the surfaces.[19,39]

Optical Bandgap Studies

UV–Visible spectrum (wavelength from 200 to 400 nm, closest to the visible range) of alkali-treated, ASA loaded, and PEG-coated Ti substrates are shown in Figs. 4a, 4b and 4c. The alkali-modified, ASA-loaded, PEG-coated Ti surfaces showed high absorbance peaks in the range 220 to 300 nm, which demonstrates

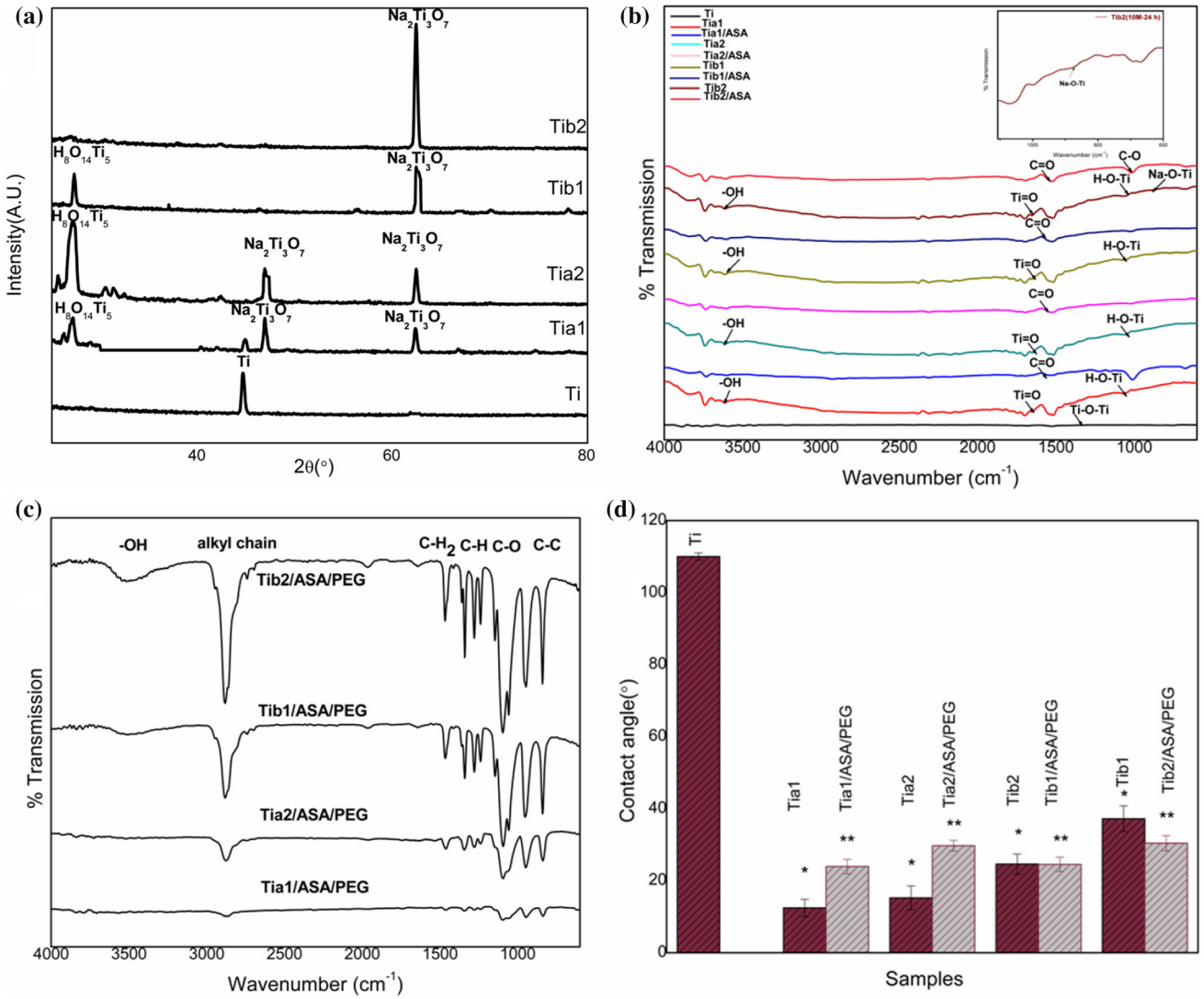

FIGURE 3. Graphical representation of (a) XRD pattern of Ti (untreated Ti), Tia1, Tia2, Tib1 and Tib2 (NaOH treated samples), (b) FTIR spectra of Tia1, Tia1/ASA, Tia2, Tia2/ASA, Tib1, Tib1/ASA, Tib2 and Tib2/ASA, a comparative study between the alkali-treated and Aspirin coated samples, (c) FTIR spectra of Tia1/ASA/PEG,Tia2/ASA/PEG,Tib1/ASA/PEG and Tib2/ASA/PEG (PEG-coated substrates) and (d) Contact angle measurement of alkali-treated substrates (Tia1, Tia2, Tib1 and Tib2) with PEG-coated sample (Tia1/ASA/PEG, Tia2/ASA/PEG, Tib1/ASA/PEG and Tib2/ASA/PEG). *$p < 0.05$ and **$p < 0.005$ relative to untreated Ti.

stronger UV light adsorption in this region. Through the encapsulation of ASA over the modified surface of Ti, the energy bandgap (E_g) has increased compared to the alkali-treated Ti substrate. The absorbance spectrum has increased after drug encapsulations are shown in Fig. 4b. In the case of PEG-coated substrates, the absorbance level decrease is smaller than the absorbance level of alkali-treated substrates and ASA loaded surface due to the high density of polymer networks over Ti substrates shown in Fig. 4c. In all the cases Tib2 (10 M-24 h) alkali-treated sample showed profound absorbance spectra.

The variation in the absorbance level is due to the increase in $Na_2Ti_3O_7$ formation on Ti substrates which has played a vital role in Aspirin encapsulation and has been observed in XRD and FTIR. The relationship between the absorbance and transmittance represented by Beer's law has shown in Eq. (2). According to Beer's Law,

$$\%T = \text{antilog}\,(2 - \text{Absorbance}) \qquad (2)$$

where $\%T$ is transmittance percentage, measures the amount of radiation absorbed by the surface.[13] Transmittance is inversely proportional to opacity. The opacity is a proportion of light occurring on the layers separated by the measure of light transmitted. In coating, this is described as the Absorbance of the coatings on the surface represented in Eq. (3), where Absorbance is opacity stated as a logarithm to base

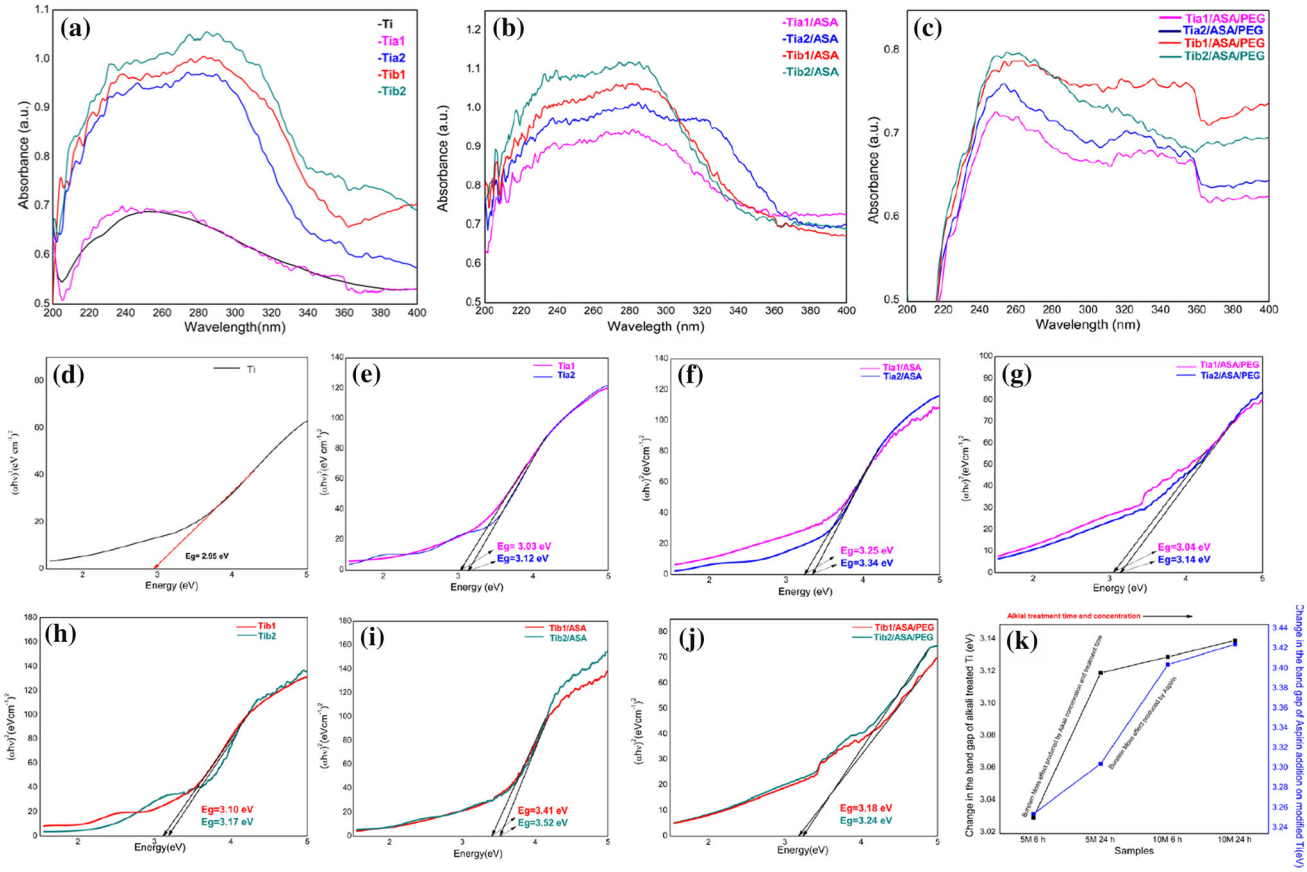

FIGURE 4. Graphical representation of Optical absorption spectra of (a) Ti (untreated cpTi), Tia1, Tia2, Tib1 and Tib2, (b) Tia1/ASA, Tia2/ASA, Tib1/ASA and Tib2/ASA and (c) Tia1/ASA/PEG, Tia2/ASA,PEG, Tib1/ASA/PEG and Tib2/ASA/PEG, Tauc plot $((\alpha h\nu)^2$ versus $h\nu$ plot for (d) Ti (untreated cpTi), For alkali treated of 5M cpTi (e) Tia1(6 h) and Tia2(24 h), (f) Aspirin(ASA) loaded cpTi- Tia1/ASA and Tia2/ASA, (g) PEG coated DES-Tia1/ASA/PEG and Tia2/ASA/PEG, For alkali treated of 10M cpTi (h) Tib1(6 h) and Tib2(24 h), (i) Aspirin(ASA) loaded cpTi-Tib1/ASA and Tib2/ASA, (j) PEG coated DES-Tib1/ASA/PEG and Tib2/ASA/PEG, and (k) General variations in the assimilation edge and bandgap of Ti substrate because of the increasing concentration and period of alkali treatment follow with the encapsulation of Aspirin.

10.[20] This estimation requires a white light source and a locator.

$$\text{Absorbance} = \log_{10}(\text{opacity}) = \log_{10}\left(\frac{1}{T}\right) \quad (3)$$

From the Table 2, we get the estimated percentage of transmittance of the incident light from the alkali-treated, ASA encapsulated, and PEG-coated cpTi surface. The intensity of light transforms when it passes through the coating surface. The pore size of the surface and the thickness of coatings played a crucial role in the transmittance percentage, thereby to the opacity of the substrate. Moreover, the absorbance is inversely related to the transmittance. The rate of light transmitted increases with the lubricious coating of PEG. Still, it is unclear regarding the optical properties of the developed composite substrates. The material is in the UV range (200–400 nm). So, the Tauc plot was calculated from the UV–visible absorbance spectrum. The Tauc plots of cpTi, alkali-treated, Aspirin loaded, and polymer-coated Ti substrates were also calculated. It has been observed from the Tauc plot that untreated Ti exhibits an energy bandgap (E_g) of 2.95 eV, which is in the lower optical energy region (semiconductive range). Alkali treatment has modified the surface, and the performance of the Ti substrate transformed it to a highly semiconductive area—redshifts observed are shown in Table 2. The variations in the energy bandgap (E_g) of the alkali-treated Ti substrates are shown in Figs. 4e and 4h. There is a continuous shift in the bandgap towards the red region on the increase in concentration time and soaking time from 3.03 to 3.12 eV for 5 M and 3.25 to 3.34 eV for 10 M NaOH treatment that shows broadening of energy bandgap. The widening of the bandgap was due to the surface nano-features. Thus, expansion of pore size leads to the enhancement of energy bandgap, thereby promoting redshift. There is a continuous change in the absorbance, absorption edge, and bandgap energy band with the increasing concentration alkali treatment

along their treatment time. The absorbance of Ti and Tia1 is about 65%, whereas, for Tia2, Tib1, and Tib2, the absorbance is almost 95, 97, and 102% (treated with 5 M-24 h, 10 M-6 h, and 10 M-24 h). The change in the absorbance leads to a redshift in the absorption edge for Tia1, Tia2, Tib1, and Tib2, along with the widening of the bandgap by 0.09 eV, 0.10 eV, and 0.11 eV. The bandgap and retention edge was evaluated utilizing the accompanying conditions given in Eq. (4) below:

$$(\alpha h\nu)^2 = \beta(h\nu - E_g) \tag{4}$$

where E_g is the optical energy bandgap and n is the power aspect of the transition forms, which depends upon the behavior of the sample. The detected red shift elucidate by the Burstein–Moss effect, consequence by the adjustment in the position of Fermi level into the conduction band. The general condition for enlargement in the energy bandgap is given by[12]:

$$\Delta E_g = \frac{h^2K^2}{2}\left[\frac{1}{m_e^*} + \frac{1}{m_h^*}\right] \tag{5}$$

where m_h^* and m_e^* are the effective proton and electron mass in the separate groups and K is Fermi wave vector shown in Eq. (5). In this situation, the move of Fermi level into the conduction band prompts the energy band enlarging as shown in Fig. 4k.

The absorption edge and the bandgap of ASA-loaded samples have similarly increased, and the redshift is more as shown in Figs. 4f and 4i. Again, enhancement in the bandgap leads to the redshift in Tia1/ASA, Tia2/ASA, and Tib1/ASA and Tib2/ASA absorption edge. The absorbance of Tia1/ASA, Tia2/ASA, Tib1/ASA, and Tib2/ASA is almost 87, 95, 100, and 110% (treated with 5 M-24 h, 10 M-6 h, and 10 M-24 h). This redshift also shifted the wavelength of the spectrum to the visible range. The shift in the absorption spectra and the energy bandgap is due to the alkali concentration and treatment time as sodium titanate formation is more in the case of 10M 24 h substrates which is also reflected in XRD FTIR and SEM. It was due to the presence of phenol hydroxyl molecular group of Aspirin on the surface, confirmed by the FTIR spectrum. Similarly, the E_g of PEG coated-Aspirin-loaded Ti substrates variations is shown in Figs. 4g and 4j.

In the case of PEG coating on Aspirin loaded alkali-treated Ti substrates, changes in the absorbance, absorption edge, and bandgap energy are observed, showing an initial blue shift in the energy band gap of 3.04 eV (Tia2/ASA/PEG) followed by a continuous redshift—3.14 eV (Tib2/ASA/PEG). Whereas, for Tib1/ASA/PEG and Tib2/ASA/PEG substrates, E_g shifts from 3.18 to 3.24 eV. It was due to the density of molecular chains associated with the high molecular weight of PEG. An intact PEG network formed over the 10 M-6 h Aspirin-loaded alkali-treated Ti substrate, as seen in SEM Fig. 2i must have shifted the energy bandgap towards the lower energy level. A porous PEG network distributed over 10 M-24 h Ti substrates, as seen in SEM micrograph (Fig. 2l), has played a crucial role in re-shifting the energy band gap again and broadening the energy bandgap. It shows that alkali concentration and treatment time have increased sodium titanate formation over cpTi, enhancing its surface, improving drug encapsulation capability, and controlling polymer network formation. So, the ASA and PEG coating on Ti exhibits non-magnetic semi-conductive behavior, which makes it compatible with the Magnetic resonance imaging (MRI) technique. However, stainless steel, cobalt–chromium, nickel–titanium, and tantalum possess an excellent electrical conductivity property. Stents manufactured from these materials can produce a "Faraday cage" effect. Faraday cage is considered a superconductor that restricts the external magnetic field and leads to diversion of the magnetic field. The cobalt–chromium alloys generate a larger magnetic field instead of absorbing them. So, stents functioning as Faraday cage can evade exterior magnetic fields to penetrate the interior bulk of the stent. It can make them less compatible with the MRI device.[70]

Drug Release Investigation and Its Mechanism

Drug-eluting behavior is an important parameter to analyze the drug release behavior and performance of the developed DES. Aspirin (ASA) as an anti-inflammatory medicine is the most utilized over-the-counter, nonsteroidal, calming medicate.[46] The thin layer of high molecular weight PEG (20,000) networking coated over the ASA-loaded alkali-treated cpTi played a crucial role in the sustainable release of the drug when it encounters the blood. The nanoporous network PEG controls the rate of release of ASA. Polymers joined with therapeutics can be bioactive to give their own practical yield or can be biodegradable to improve drug discharge rate and avert transporter aggregation. The effect of drug quantity on the delivery profile was examined. Moreover, the release of the drug depends upon the type of association between the drug and PEG. The experimental information fitted well to the Ritger–Peppas mathematical equation, and the diffusion exponent n was additionally determined to dissect the delivery pattern. The feature outcomes are shown in Fig. 5 and Table 3.

Drug loading is also a significant cause of ASA delivery. It is mainly based on the quantity of ASA and the dimension of the substrate. The dose of 50 mg/100 mm^2 shows moderate drug discharge compared to an amount of 150 mg/100 mm^2. However, low dose ASA

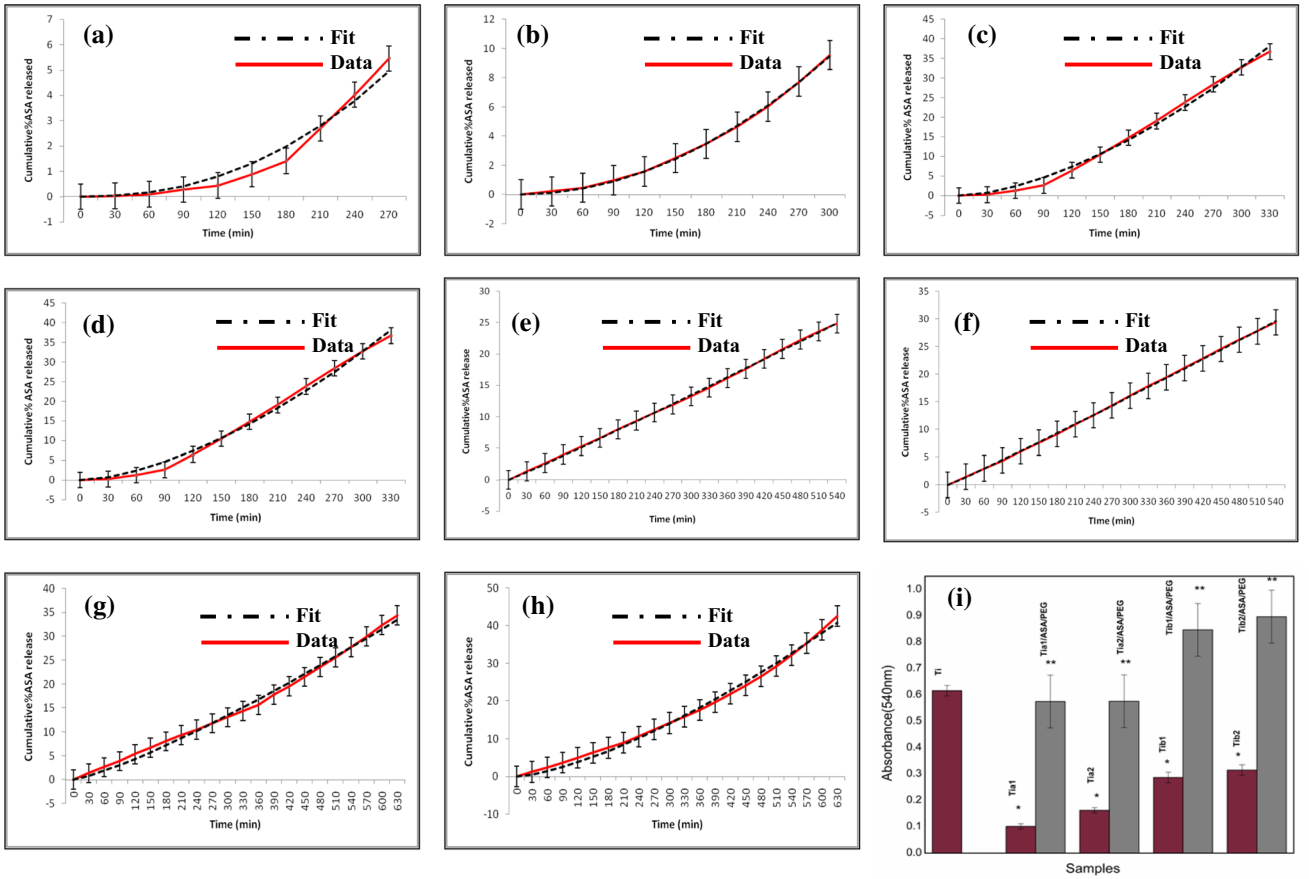

FIGURE 5. Ritger-Peppas model kinetic release of the ASA 50 mg dose—(a) Tia1/ASA/PEG, (b) Tia2/ASA/PEG, (c) Tib1/ASA/PEG, (d) Tib2/ASA/PEG, 150 mg dose- (e) Tia1/ASA/PEG, (f) Tia2/ASA/PEG, (g) Tib1/ASA/PEG, (h) Tib2/ASA/PEG and Bar graph showing the representation of (i) Antithrombotic assay of alkali-treated sample. Here, Tib2 has higher absorbance compare to the Tia1, Tia1/ASA/PEG, Tia2, Tia2/ASA/PEG, Tib1, Tib1/ASA/PEG, Tib2 and Tib2/ASA/PEG. **$p < 0.005$ and *$p < 0.05$ relative to Ti substrate (Control).

TABLE 3. Constants determined from fitting the information of Aspirin (ASA) release to the Ritger–Peppas condition.

	Sample							
	50 mg dose				150 mg dose			
Ritger–peppas constant	Tia1/ASA/PEG	Tia2/ASA/PEG	Tib1/ASA/PEG	Tib2/ASA/PEG	Tia1/ASA/PEG	Tia2/ASA/PEG	Tib1/ASA/PEG	Tib2/ASA/PEG
n	2.26	1.95	1.63	1.55	1.04	1.05	1.23	1.43
R^2	0.990	0.999	0.997	0.993	0.999	0.999	0.998	0.998

(50 mg/100 mm^2) was released for 330 min as shown in Figs. 5c and 5d whereas high dose ASA (150 mg/100 mm^2) was released for 630 min shown in Figs. 5g and 5h. No initial burst release was observed for 50 mg loaded substrates. For 120 min, the ASA release was slow due to the polymer layer's degradation. Later, the elution rate escalated, which may be due to its hydrophilic behavior, as inferred from the FTIR graph. It increases the absorption of water molecules.[10]

The release profile also demonstrates that an increase in treatment time and concentration has played a vital parameter in modifying the surface, thereby improving the ASA loading capacity of the substrates and polymer network formation over it. High drug contents are more likely to encapsulate within the nano-pores than low amounts of drugs. In addition, high dose ASA creates concentration gradient and osmotic pressure (driving strength), which accelerate

drug release. Cumulative release percentage of 150 mg dose samples—Tia1/ASA/PEG is 24.3 ± 1.5%, Tia2/ASA/PEG is 29.3 ± 3.0%, Tib1/ASA/PEG is 34.4 ± 2.0% and Tib2/ASA/PEG is 42.6 ± 2.5%. In addition, cumulative release percentage 50 mg dose samples—Tia1/ASA/PEG is 5.5 ± 3.2%, Tia2/ASA/PEG is 9.5 ± 3.0%, Tib1/ASA/PEG is 36 ± 1.5% and Tib2/ASA/PEG is 38 ± 1.4%. Overall, the cumulative drug release percentage is 42.6 ± 2.5%, which is less than 60% of drug release. Therefore, the kinetic model fitted with Ritger–Peppas mathematical model equation. Moreover, when the concentration of ASA increased (tripled-150 mg), as shown in Fig. 5h, the drug release profile was extended beyond 10 h. The drug release studies of Tib2/ASA/PEG shows superior in elution without any initial burst performing a sustained release behavior compared to other substrates. However, initial burst release was observed for all 150 mg dose-loaded substrates. It may be due to the presence of ASA crystal on the substrate's surface. This result is in line with the literature, which demonstrated an initial burst release due to the surface integrated drug. The initial burst release is effective in initial treatment by inhibiting thrombosis.[10] The linear release study shows the bioavailability of ASA as aspirin instantly interacts with the arterial thrombosis site without any systemic circulation. It also reduces the side effects of the ASA on other organs. Earlier studies stated the bioavailability of different doses of ASA (20, 40, 325, and 1300 mg) and concluded that the bioavailability is almost 40–50% in the systemic circulation. The study also revealed that a low dosage of ASA shows a maximum decrease in thrombosis before detection of ASA in the systemic circulation.[38]

Therefore, the results suggest that surface treatment has enhanced the drug loading capability of the substrates, and the polymer network formed over it has aided the controlled release. Still, the release period *in-vitro* is only 10 h, significantly less. It was due to the thickness of PEG coating (bare), a layer of coating, its adherence with the cpTi substrates, and the pH of the medium. In general, Surface modification is a crucial parameter in improving the morphology of cpTi substrates and enhancing the drug loading capabilities by strengthening the hydrophilic nature of the substrates. Therefore, tailoring the surface features and controlling the polymer coating are the most challenging parameters that reflect the drug elution pattern.

As summed up in Table 3, each R^2 was determined to be higher than 0.98, signifying that the experimental information coordinated well with the observational condition. The diffusion constant n specifies the technique of medication discharge. The n value of each composite is greater than or equal to 1, which means ASA is diffusing from cpTi substrate following Super case II transport mechanism. The impact of polymer chain relaxation played a vital role in the conveyance of the medication, prompting a nearly Case II transport mechanism. However, the effect of pH also transpired in this mechanism and played a vital role in the medication transport system. These perceptions are identified with the anionic attributes of the PEG polymer (MW 20,000) structure. The macromolecules chain relaxation of high molecular weight polymer dominates the driving strength. An increase in the pH of the delivery medium brought about the ionization of the carboxylic gatherings in the methacrylate structure of PEG and the subsequent aversion between polymer chains. Afterward, broad ionization of the functional group at pH 7.4 effectively affected the polymer chain relaxation and, thus, the medication transport component.[40] Consequently, the Super case II transport mechanism was observed at pH 7.4. PEG coating also gets degrades with pH change and hydrolytic effect.

Antithrombotic Assay

The antithrombotic assay has carried over the developed DES to analyze the effect of alkali treatment on thrombosis generation, which is important for stent implants. The UV absorbance range has shown in Fig. 5i; lower the absorbance implies fewer RBCs in the hemoglobin arrangement.[61] Absorbance for the PEG-coated sample such as Tia1/ASA/PEG, Tia2/ASA/PEG, Tib1/ASA/PEG and Tib2/ASA/PEG were about 0.575 ± 0.1, 0.576 ± 0.1, 0.847 ± 0.1 and 0.897 ± 0.1. It is evident from the graph that 10 M-24 h PEG-coated Ti substrate (Tib2/ASA/PEG) has more absorbance. It means higher the absorbance more number of RBCs present in the blood than the surface. It may be due to the presence long molecular chain of PEG, which reduces the thrombosis formation.[5] Therefore, the coagulation efficiency is more in a lower concentration of the alkali-treated sample, as sodium titanate formation and aspirin encapsulation are less. On the other hand, by increasing the alkali concentration and its treatment time, the coagulation efficiency decreases due to improved surface features created by sodium titanate—aspirin aggregation. It may be due to the more negative groups (demonstrated in the FTIR graph), which repels the net negative charges of the blood platelets. This negative-negative charge highly repels and thereby prevents thrombosis formation. Hence, the alkali and aspirin treatment concentration plays an important role in controlling the thrombosis generation over DES. Aspirin is a highly potent molecule in inhibiting cardiovascular disease in patients. It impedes platelet gathering on the substrate's surface by diminishing thromboxane A2 formation. Thus, it helps in preventing the damage of

the arterial wall. It was demonstrated that maximum platelet COX-1 suppressed and minimizes the platelet thromboxane A2 with a low dose of ASA. A previous study reported that a 30 mg/day dose of ASA minimizes the thrombosis development in healthy volunteers. Similarly, the ASA dose of 75 mg/day and 300 mg/day was also demonstrated to lessen the thrombin to the same range. However, its effectiveness started to decrease with high dosage, i.e., beyond 500 mg in healthy volunteers.[35,63] Further, it has been found that 75 mg/day is insignificant in reducing the thrombosis in the patient, whose cholesterol level is between 200 and 250 mg/dL.[42] Hence, loading of 150 mg dose of ASA is considered to be safe to counteract the effect of high dosage and overcoming the limitations of low dose of ASA (50 mg).

CONCLUSION

The present work reports the development of multifunctional cpTi-drug-eluting substrates fabricated from cpTi with alkali treatment. The treatment time and concentration of NaOH configured sodium titanate oxide layer, which evoked surface nanometers, played a crucial role by modifying the surface morphologies of cpTi substrates and enhancing its drug loading capacity. The NaOH treatment alters the surface chemistry of cpTi, which facilitates the binding of ASA and PEG. The hydrophilic nature of ASA was also revealed through contact angle measurement. Surface treatment has broadened the energy bandgap, improving the semiconductive property of developed DES. Also, the non-covalent PEG (20,000) coating maintains the optical feature by continuously shifting towards higher energy. The initial burst release was not found for a low dose of ASA (50 mg), whereas burst release accelerated with a high amount of ASA (150 mg). The drug release kinetics was best fitted with Ritger–Peppas mathematical model equation ($R^2 > 0.98$) and diffusion exponent, n value was found to be greater than 1 signifies super case II transport mechanism behind the release of ASA from cpTi substrates. The initial burst release of ASA from Tib2/ASA/PEG (150 mg dose) with an absorbance value of 0.897 ± 0.1 showed a more considerable decrease in blood clot formation than other developed DES. Further, a longer molecular chain of PEG also reduces thrombosis formation. Therefore, this investigation provides insight by countering the restriction of cpTi through surface treatment with alkali (NaOH), the embodiment of drug (Aspirin), and coating with polymer (PEG) network.

CONFLICT OF INTEREST

THE AUTHORS DECLARE NO CONFLICT OF INTEREST.

ETHICAL APPROVAL

This article does not contain any studies with human participants or animals performed by any of the authors.

REFERENCES

[1]Abazovic, N. D., M. I. Comor, C. Mirjana, M. D. Dramicanin, D. J. Jovanovic, S. P. Ahrenkiel, and J. M. Nedeljkovic. Photoluminescence of anatase and rutile TiO_2 particles. *J. Phys. Chem. B*. 110:25366–25370, 2006.

[2]Abdelamir, A. I., E. A. Bermany, and F. S. Hashim. Enhance the optical properties of the synthesis PEG/Graphene- based nanocomposite films using GO nanosheets. *J. Phys. Conf. Ser*.1294:022029, 2019.

[3]Abouelmagd, S. A., B. Sun, A. C. Chang, Y. J. Ku, and Y. Yeo. Release kinetics study of poorly water-soluble drugs from nanoparticles: are we doing it right? *Mol. Pharm*. 12:997–1003, 2015.

[4]Acharya, G., R. A. Hopkins, and C. H. Lee. Advanced polymeric matrix for valvular complications. *J. Biomed. Mater. Res. A*. 100:1151–1159, 2012.

[5]Alibeik, S., S. Zhu, and J. L. Brash. Surface modification with PEG and hirudin for protein resistance and thrombin neutralization in blood contact. *Coll. Surf. B Biointerfaces*. 81:389–396, 2010.

[6]Anisha, A. D., and R. Shegokar. Polyethylene glycol (PEG): a versatile polymer for pharmaceutical applications. *Expert Opin. Drug Deliv*. 13:1257–1275, 2016.

[7]Arcoria, A., E. Maccarone, G. Musumarra, and G. A. Tomaselli. Ultraviolet and infrared absorption spectra of 2-thiophenesulfonamides. *Spectrochim. Acta A Mol. Biomol. Spectrosc*. 30:611–618, 1974.

[8]Arvidson, K., M. Cottler-fox, E. Hammarlund, and U. L. F. Friberg. Cytotoxic effects of cobalt-chromium alloys on fibroblasts derived from human gingiva. *Scand. J. Dent. Res*. 95:356–363, 1987.

[9]Baker, A., U. Nautiyal, M. S. Kumar, and B. Bhusan. Polymeric systems as controlled release drug products: a review. *Int. J. Pharm. Med. Res*. 2:72–77, 2014.

[10]Basnett, P., K. Y. Ching, M. Stolz, J. C. Knowles, A. R. Boccaccini, C. Smith, I. C. Locke, and I. Roy. Aspirin-loaded P(3HO)/P(3HB) blend films: potential materials for biodegradable drug-eluting stents. *Bioinspir. Biomim. Nanobiomater*. 2:141–153, 2013.

[11]Bhachu, D. S., S. Sathasivam, G. Sankar, D. O. Scanlon, G. Cibin, C. J. Carmalt, I. P. Parkin, G. W. Watson, S. M. Bawaked, A. Y. Obaid, S. A. Thabaiti, and S. N. Basahel. Solution processing route to multifunctional titania thin films: highly conductive and photcatalytically active Nb:TiO_2. *Adv. Funct. Mater*. 24:5075–5085, 2014.

[12]Bharti, B., S. Kumar, H. Lee, and R. Kumar. Formation of oxygen vacancies and Ti_3^+ state in TiO_2 thin film and enhanced optical properties by air plasma treatment. *Sci. Rep*. 6:32355, 2016.

[13]Bishop, C. Process Diagnostics and Coating Characteristics. Vacuum Deposition onto Webs, Films and Foils. Amsterdam: Elsevier, 2007.
[14]Boehlert, C. J., C. J. Cowen, J. P. Quast, T. Akahori, and M. Niiomi. Fatigue and wear evaluation of Ti-Al-Nb alloys for biomedical applications. *Mater. Sci. Eng. C*. 28:323–330, 2008.
[15]Bridgeman, J. T., V. A. Marker, S. K. Hummel, B. W. Benson, and L. L. Pace. Comparison of titanium and cobalt-chromium removable partial denture clasps. *J. Prosthet. Dent*. 78:187–193, 1997.
[16]Buecker, A., J. M. Neuerburg, G. B. Adam, A. Glowinski, T. Schaeffter, V. Rasche, J. J. V. Vaals, A. M. Nielsen, and R. W. Guenther. Real-time MR fluoroscopy for MR-guided iliac artery stent placement. *J. Magn. Reson. Imaging*. 12:616–622, 2000.
[17]Buriuli, M., W. G. Kumari, and D. Verma. Evaluation of hemostatic effect of polyelectrolyte complex- based dressings. *J. Biomater. Appl*. 32:638–647, 2017.
[18]Campuzano, S., M. Pedrero, P. Y. Sedeno, and J. M. Pingarron. Antifouling (Bio)materials for electrochemical (Bio)sensing. *Int. J. Mol. Sci*. 20:423, 2019.
[19]Chen, H., X. Hu, Y. Zhang, D. Li, Z. Wu, and T. Zhang. Effect of chain density and conformation on protein adsorption at PEG-grafted Polyeurethane surfaces. *Coll. Surf. B: Biointerfaces*. 61:237–243, 2008.
[20]Chou, J., T. J. Robinson, and H. Doan. Rapid comparison of UVB absorption effectiveness of various sunscreens by UV-Vis spectroscopy. *J. Anal. Bioanal. Technol*. 8:355, 2017.
[21]Ciobanu, G., G. Carja, O. Ciobanu, I. Sandu, and A. Sandu. SEM and EDX studies of bioactive hydroxyapatite coatings on titanium implants. *Micron*. 40:143–146, 2009.
[22]Domtau, D. L., J. Simiyu, E. O. Ayieta, G. M. Asiimwe, and J. M. Mwabora. Influence of pore size on the optical and electrical properties of screen printed TiO_2 thin films. *Adv. Mater. Sci. Eng*. 2016:7515802, 2016.
[23]Gunasekaran, S., R. K. Natarajan, V. Renganayaki, and S. Natarajan. Vibrational spectra and thermodynamic analysis of metformin. *Indian J. Pure Appl. Phys*. 44:495–500, 2006.
[24]Gunn, J., and D. Cumberland. Stent coatings and local drug delivery State of the art. *Eur. Heart J*. 20:1693–1700, 1999.
[25]Guo, Z., N. Jiang, C. Chen, S. Zhu, L. Zhang, and Y. Li. Surface bioactivation through the nanostructured layer on titanium modified by facile HPT treatment. *Sci. Rep*. 7:4155, 2017.
[26]Guo, Y., B. Wu, Y. Hu, R. Zuo, X. Lu, S. Xiong, and P. Huang. Osteogenic properties of bioactive sodium titanate/titanium oxide composite coating prepared by anodic oxidation in NaOH electrolyte. *New J. Chem*. 45:8572–8581, 2021.
[27]Han, Y., B. Xu, Q. Jing, S. Lu, L. Yang, K. Xu, Y. Li, J. Li, C. Guan, A. J. Kirtane, and Y. Yang. A randomized comparison of novel biodegradable polymer- and durable polymer-coated cobalt-chromium sirolimus-eluting stents. *J. Am. Coll. Cardiol. Interv*. 7:1352–1360, 2014.
[28]Hanib, N. H., F. Hamzah, Z. Omar, and I. Subuki. Surface characterization onalkali-heat-treatment on titanium alloy. *Malays. J. Anal. Sci*. 20:1429–1436, 2016.
[29]Hui, N., X. Sun, S. Niu, and X. Luo. PEGylated polyaniline nanofibers: antifouling and conducting biomaterial for electrochemical DNA sensing. *ACS Appl. Mater. Interfaces*. 9:2914–2923, 2017.
[30]Iwunze, M. O. Absorptiometric determination of acetylsalicylic acid in aqueous ethanolic solution. *Anal. Lett*. 41:2944–2953, 2008.
[31]Jemat, A., M. J. Ghazali, M. Razali, and Y. Otsuka. Surface modifications and their effects on titanium dental implants. *Biomed. Res. Int*.2015:791725, 2015.
[32]Jian, M. K., W. P. Chen, M. Feng, and H. B. Zhan. Controlled release of aspirin from SiO_2-PEG hybrid coating on 316LSS substrate for the preparation of drug eluting stents. *J. Adv. Mater. Res*. 287:1956–1959, 2011.
[33]Karlsson, J., S. Atefyekta, and M. Andersson. Controlling drug delivery kinetics from mesoporous titania thin films by pore size and surface energy. *Int. J. Nanomed*. 10:4425–4436, 2015.
[34]Kim, C., M. R. Kendall, M. A. Miller, C. L. Long, P. R. Larson, M. B. Humphrey, A. S. Madden, A. C. Tas, H. T. Varghese, C. Y. Panicker, and D. Philip. Comparison of titanium soaked in 5 M NaOH or 5 M KOH solutions. *Mater. Sci. Eng. C Mater. Biol. Appl*. 33:327–339, 2013.
[35]Kyrle, P. A., J. Westwick, M. F. Scully, V. V. Kakkar, and G. P. Levis. Investigation of the interaction of blood platelets with the coagulation system at the site of plug formation ex vivo in man: effect of low-dose aspirin. *Thromb. Haemost*. 57:62–69, 1987.
[36]Li, D., P. Lv, L. Fan, Y. Huang, F. Yang, X. Me, and D. Wu. The immobilization of antibiotic-loaded polymeric coatings on osteoarticular Ti implants for the prevention of bone infections. *Biomater. Sci*. 5:2337–2346, 2017.
[37]Liu, H., L. Du, Y. Zhao, and W. Tian. In vitro hemocompatibility and cytotoxicity evaluation of halloysite nanotubes for biomedical application. *J. Nanomater*.2015:685323, 2015.
[38]Maulidiyah, H. Ritonga, C. E. Faiqoh, D. Wibowo, and M. Nurdin. Preparation of TiO_2-PEG thin film on hydrophilicity performance and photocurrent response. *Biosci. Biotechnol. Res. Asia*. 12:1985–1989, 2015.
[39]Medendorp, C. A., S. Parkin, and T. Li. The confusion of indexing aspirin crystals. *J. Pharm. Sci*. 97:1361–1367, 2008.
[40]Meek, I. L., M. A. F. J. Vandelar, and H. E. Vonkeman. Non-steroidal anti-inflammatory drugs: an overview of cardiovascular risks. *Pharmaceuticals*. 3:2146–2162, 2010.
[41]Mohanta, M., and A. Thirugnanam. Drug release studies of titanium based polyethylene glycol coating as multifunctional substrate. *Mater. Today: Proc*. 47:257–260, 2021.
[42]Musial, J., A. Undas, R. Undas, J. Brozek, and A. Szczeklik. Treatment with simvastatin and low-dose aspirin depresses thrombin generation in patients with coronary heart disease and borderline-high cholesterol levels. *Thromb. Haemost*. 85:221–225, 2001.
[43]Naghibi, S., H. R. M. Hosseini, M. A. F. Sani, M. A. Shokrgozar, and M. Mehrjoo. Mortality response of folate receptor-activated, PEG–functionalized TiO_2 nanoparticles for doxorubicin loading with and without ultraviolet irradiation. *Ceram. Int*. 40:5481–5488, 2014.
[44]Ozcelik, B., K. D. Brown, A. Blencowe, K. Ladewig, G. W. Stevens, J. P. Scheerlinck, K. Abberton, M. Daniell, and G. G. Qiao. Biodegradable and biocompatible poly(ethylene glycol)-based hydrogel films for the regeneration of corneal endothelium. *Adv. Healthc. Mater*. 3:1496–1507, 2014.
[45]Pacetti, S. D., S. Jose, P. A. Kramer-Brown, R. J. Santos, J. W. Morris, and S. M. Malik, MRI compatible, radiopaque alloys for use in medical devices. Pub. No .: US 2008 / 0195194A1.2008. pp. 1-10.

[46]Pedersen, A. K., and G. A. FitzGerald. Dose-related kinetics of aspirin. Presystemic acetylation of platelet cyclooxygenase. *N. Engl. J. Med.* 311:1206–1211, 1984.
[47]Prencipe, G., S. K. Tabakman, K. Welsher, Z. Liu, H. Dai, A. P. Goodwin, L. Zhang, J. Henry, and H. Dai. PEG branched polymer for functionalistaion of nanomaterials with ultralong blood circulation. *J. Am. Chem. Soc.* 131:4783–4787, 2009.
[48]Qi, P., M. F. Maitz, and N. Huang. Surface modification of cardiovascular materials and implants. *Surf. Coat. Technol.* 233:80–90, 2013.
[49]Reejhsinghani, R., and A. S. Lotfi. Prevention of stent thrombosis: challenges and solutions. *Vasc. Health Risk Manag.* 11:93–106, 2015.
[50]Riberiro, L. S., L. F. Gorup, F. F. B. Silva, C. Ribeiro, and E. R. Camargo. New approach of the oxidant peroxo method (OPM) route to obtain $Ti(OH)_4$ nanoparticles with high photocatalytic activity under visible radiation. *Int. J. Photoenergy*. 2018:6098302, 2018.
[51]Saeed, M., S. W. Hetts, J. English, and J. M. Wilson. MR fluoroscopy in vascular and cardiac interventions (review). *Int. J. Cardiovasc. Imaging*. 28:117–137, 2012.
[52]Selden, A. I., B. Persson, S. I. Bornberger-dankvardt, and L. E. Winstrm. Exposure to cobalt chromium dust and lung disorders in dental technicians. *Thorax*. 50:769–772, 1995.
[53]Serra, L., J. Domenech, and N. A. Peppas. Drug transport mechanisms and release kinetics from molecularly designed poly(acrylic acid-G-ethylene glycol) hydrogels. *Biomaterials*. 27:5440–5451, 2006.
[54]Serruys, P. W., S. Garg, and A. Abizaid. A randomized comparison of novolimus-eluting andzotarolimus-eluting coronary stents: 9-month follow-up results of the EXCELLA II study. *EuroIntervention*. 6:195–205, 2010.
[55]Shih, C. C., C. M. Shih, Y. Y. Su, and S. J. Lin. Impact on the thrombogenicity of surface oxide propertiesof 316l stainless steel for biomedical applications. *J. Biomed. Mater. Res. A*. 67:1320–1328, 2003.
[56]Silverstein, R. M., and G. C. Bossier. Spectrometric identification of organic compounds. *J. Chem. Educ.* 39:546, 1962.
[57]Suwanprateeb, J., and F. Thammarakcharoen. Influence of surface pretreatment on the coating quantity and properties of nanostructured octacalcium phosphate on commercially pure titanium. *Indian J. Eng. Mater. Sci.* 24:351–361, 2017.
[58]Tartaglia, J. M., J. P. Loeffler, and T. H. Turnlund, Polymer film for wrapping a stent structure. United States Patent (19) Patent Number: 5700286, 1997.
[59]Thirugnanam, A., T. S. S. Kumar, and U. Chakkingal. Bioactivity enhancement of commercial pure titanium by chemical treatments. *Trends Biomater. Artif. Organs*. 23:76–85, 2009.
[60]Thomas, A., S. S. Muller, and H. Frey. Beyond poly(-ethylene glycol): linear polyglycerol as amultifunctional polyether for biomedical and pharmaceutical applications. *Biomacromolecules*. 15:1935–2195, 2014.
[61]Totea, G., D. Ionita, I. Demetrescu, and M. M. Mitache. *In-vitro* hemocompatibility and corrosion behavior of new Zr-binary alloys in whole human blood. *Cent. Eur. J. Chem.* 12:796–803, 2014.
[62]Uhrich, K. E., S. M. Cannizzaro, R. S. Langer, and K. M. Shakesheff. Polymeric systems for controlled drug release. *Chem. Rev.* 99:3181–3198, 1999.
[63]Undas, A., R. Undas, J. Musial, and A. Szczeklik. A low dose of aspirin (75 mg/day) lowers thrombin generation to a similar extent as a high dose of aspirin (300 mg/day). *Blood Coagul. Fibrinolysis*. 11:231–234, 2000.
[64]Varghese, H. T., C. Y. Panicker, and D. Philip. Vibrational spectroscopic studies and ab initio calculations of sulfanilamide. *Spectrochim. Acta A Mol. Biomol. Spectrosc.* 65:155–158, 2006.
[65]Venkatasubbu, G. D., S. Ramasamy, V. Ramakrishnan, and J. Kumar. Folate targeted PEGylated titanium dioxide nanoparticles as a nanocarrier for targeted paclitaxel drug delivery. *Adv. Powder Technol.* 24:947–954, 2013.
[66]Viceconti, M., R. Muccini, M. Bernakiewicz, M. Baleani, and L. Cristofolini. Large-sliding contact elements accurately predict levels of bone implant micromotion relevant to osseointegration. *J. Biomech.* 33:1611–1618, 2000.
[67]Walker, J. A., K. J. Robinson, C. Munro, T. Gengenbach, D. A. Muller, P. R. Young, L. H. L. Lua, and S. R. Corrie. Antibody-binding, antifouling surface coatings based on recombinant expression of Zwitterionic EK peptides. *Langmuir*. 35:1266–1272, 2019.
[68]Wei, M., H. Kim, T. Kokubo, and J. H. Evans. Optimising the bioactivity of alkaline-treated titanium alloy. *Mater. Sci. Eng.* 20:125–134, 2002.
[69]Wijns, W., M. Vrolix, S. Verheye, and D. Schoors. Long-term clinical outcomes of a crystalline sirolimus-eluting coronary stent with a fully bioabsorbable polymer coating: five-year outcomes from the DESSOLVE I and II trials. *EuroIntervention*. 13:e2147–e2151, 2018.
[70]Xu, Y., and R. Yu. Comparison of magnetic resonance imaging artifacts of five common dental materials. *Hua Xi Kou Qiang Yi Xue Za Zhi*. 33:230–233, 2015.
[71]Yadav, M. D. Advanced Nanocomposite Ion Exchange Materials for Water Purification. Handbook of Nanomaterials for Wastewater Treatment. Amsterdam: Elsevier, pp. 513–534, 2021.
[72]Yang, K., and Y. Ren. Nickel-free austenitic stainless steels for medical applications. *Sci. Technol. Adv. Mater.*11:014105, 2010.
[73]Zhang, Q., J. P. Yang, J. Hu, A. J. Kirtane, T. Q. Zhu, R. Y. Zhang, Z. K. Yang, J. Hu, F. H. Ding, R. Du, and W. F. Shen. Comparison of biodegradable polymer versus durable polymer Sirolimus-Eluting stenting in patients with acute ST-Elevation myocardial infarctionundergoing primary percutaneous coronary intervention: results of the RESOLVE study. *J. Interv. Cardiol.* 27:131–141, 2014.
[74]Zhang, X. I. N., L. I. C. Wei, B. I. N. Wu, L. I. Y. Yu, X. P. Wang, and Y. U. E. Liu. A comparative analysis of metal allergens associated with dental alloy prostheses and the expression of HLA-DR in gingival tissue. *Mol. Med. Rep.* 13:91–98, 2016.
[75]Zhang, X., G. Zhang, H. Zhang, J. Li, X. Yao, and B. Tang. Surface immobilization of heparin and chitosan on titanium to improve hemocompatibility and antibacterial activities. *Coll. Surf. B Biointerfaces*. 172:338–345, 2018.